

## 8. HABITABILITY OF SUBSEAFLOOR SEDIMENTS AT THE COSTA RICA CONVERGENT MARGIN<sup>1</sup>

D. Cardace,<sup>2</sup> J.D. Morris,<sup>2</sup> A.D. Peacock,<sup>3</sup> and D.C. White<sup>3</sup>

### ABSTRACT

Assessing the habitability of deep-sea sediments undergoing compaction, compression, and subduction at convergent margins adds to our understanding of the limits of the terrestrial biosphere. In this work, we report exploratory biomarker data on sediments obtained at Ocean Drilling Program (ODP) Sites 1253, 1254, and 1255 during drilling at the Costa Rica subduction trench and forearc sedimentary wedge. The samples selected for postcruise biomarker analyses were located within intervals of potentially enhanced fluid flow within the décollement and sedimentary wedge fault zones (Sites 1254 and 1255) and within basal carbonates at the reference site (Site 1253). The passage of fluids that are geochemically distinct from ambient interstitial water provides a disequilibrium setting that may enhance habitability. Biomarker data show low levels of microbial biomass in subseafloor sediments sampled at the Costa Rica convergent margin as deep as ~370 meters below seafloor.

### INTRODUCTION

The extent of Earth's deep biosphere is a great unknown in biogeochemistry. Historically perceived as barren, the deep subseafloor is now understood to host a persistent biota, with conditions that can sustain microbial life extending to several kilometers depth (Parkes et al., 2000). The amount of prokaryotes inhabiting the oceanic subsurface alone (estimated at  $355 \times 10^{28}$  cells, equivalent to ~303 Pg [ $1 \times 10^{15}$  g] of

<sup>1</sup>Cardace, D., Morris, J.D., Peacock, A.D., and White, D.C., 2006. Habitability of subseafloor sediments at the Costa Rica convergent margin. In Morris, J.D., Villinger, H.W., and Klaus, A. (Eds.), *Proc. ODP, Sci. Results*, 205, 1–26 [Online]. Available from World Wide Web: <[http://www-odp.tamu.edu/publications/205\\_SR/VOLUME/CHAPTERS/213.PDF](http://www-odp.tamu.edu/publications/205_SR/VOLUME/CHAPTERS/213.PDF)>. [Cited YYYY-MM-DD]

<sup>2</sup>Washington University, One Brookings Drive, Campus Box 1169, St. Louis MO 63130-4899, USA. Correspondence author: [dcardace@wustl.edu](mailto:dcardace@wustl.edu)

<sup>3</sup>Center for Biomarker Analysis, The University of Tennessee Knoxville, 10515 Research Drive, Suite 300, Knoxville TN 37932-2575, USA.

carbon) surpasses other environments on Earth by far (Whitman et al., 1998).

The Integrated Ocean Drilling Program (IODP) sees the investigation of the deep biosphere as one of its major research initiatives, building on numerous pioneering studies of deep seafloor ecosystems that emerged from science associated with Ocean Drilling Program (ODP) expeditions. A ground-breaking and impressive array of projects aimed at exploring seafloor sediments resulted from ODP Leg 201, which cored a number of complementary seafloor environments at the Peru margin, which are relevant to this study along the Middle America Trench. An incredible diversity of metabolic strategies employed in the deep subsurface have been documented (D'Hondt et al., 2004, and references therein). Productive work continues on sediment cores obtained during Leg 201, including bacterial deoxyribonucleic acid (DNA) sequencing and radiotracer studies of bacterial metabolic reaction rates (Schippers et al., 2005). In addition, Parkes et al. (2005) found that microbial activity was enhanced at geological interfaces in the subsurface and generated a changing microbial ecology with depth below seafloor, related to the geochemistry of interstitial pore fluids and the availability of electron donors and acceptors. Finally, evidence is mounting that heterotrophic Archaea may be active in the Leg 201 study area; Biddle et al. (2006) use a rich 16S ribosomal ribonucleic acid (rRNA) data set combined with stable isotope data for Archaeal cells, Archaeal membrane components, and ambient sedimentary organic matter to infer that both anaerobic oxidation of methane and degradation of refractory organic carbon are ongoing in the seafloor off Peru.

There is particular potential for life associated with convergent tectonic plate boundaries. Seafloor sediments cored at the Nankai Trough during ODP Leg 190 showed persistent prokaryotic biomass and evidence for methanogenesis (Newberry et al., 2004) and also yielded cultivable bacteria from several meters below seafloor (Toffin et al., 2004). Studies of samples of Mariana forearc serpentine mud volcanoes, recovered from ODP Site 1200, have clarified how alkaliphilic bacteria can take advantage of the mixing of seawater and upwelling alkaline solutions in the seafloor (Takai et al., 2005). At Costa Rica, the convergent margin sedimentary cover hosts gas hydrate (Schmidt et al., 2005) and is linked to methane-cycling microbial life and cold seep communities dependent on deeply sourced fluid venting from complex fault networks associated with tectonic compression (Mau et al., 2006). Coring during ODP Leg 205 allowed collection of sediment samples near a modern subduction trench, enabling us to conduct a suite of biomarker analyses in an area well described by previous coring (ODP Leg 170).

Leg 205 science planning involved two predominant scientific themes: (1) to clarify the igneous character and alteration history of the mafic complex at ODP Site 1253 and (2) to describe hydrologic systems in the igneous section and in fault zones at ODP Sites 1254 and 1255. In both themes, microbial processes that alter solid and fluid phase chemistries could play a significant role. Microbes can transform biologically important metals in both solid and liquid phases, catalyzing reduction or oxidation reactions at accessible mineral surfaces. Microbes also impact ambient fluid chemistry by intake and excretion of chemical species, potentially impacting the geochemistry of interstitial and formation fluids. The potential for microbial impacts underscores the need to characterize microbial community structure and diversity in the seafloor sediments offshore Costa Rica.

In this work, we report biomarker data on sediments obtained at Sites 1253, 1254, and 1255 near the Costa Rica subduction trench. Cellular components extracted from lyophilized sediment were analyzed for microbial (1) ester-linked phospholipid fatty acids (PLFA), (2) DNA, (3) methanogen gene copy numbers, and (4) respiratory quinones.

## **GEOLOGICAL SETTING**

The subduction of the Cocos plate beneath the Caribbean plate generates the Middle America Trench and the Central America volcanic arc. During Legs 205 and 170, deep-sea sediment cores were recovered from the sedimentary blanket on the Cocos and Caribbean plates offshore of the Nicoya Peninsula, where early Miocene-age (~24 Ma) oceanic crust is currently subducting along the Middle America Trench at ~79 mm/yr (DeMets et al., 1990) (Fig. F1). Figure F2 provides a seismic reflection profile showing the subduction of the incoming plate and its sedimentary blanket, with cored sites and relevant sedimentary features indicated (Shipboard Scientific Party, 2003a). In brief, sediment and rock cored at the reference site (Sites 1039/1253) encompass a mafic igneous complex, overlain by ~270 m of calcareous ooze with evidence for hydrothermal alteration at its base, and ~70 m of hemipelagic silty clay, topped by ~80 m of diatomaceous ooze with ash-rich and sandy intervals. Sites 1040/1254 and 1043/1255 cored through the forearc wedge toe, recovering as much as ~370 m of sedimentary wedge sediments composed of mass-wasted continental margin material above the décollement, below which incoming sediments subduct.

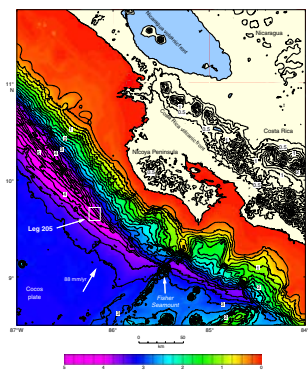
During sediment subduction, deep-sea microbial communities in incoming sediments experience a new environment dominated by compaction dewatering and through-flow of deeply sourced fluids. At present we are interested in documenting viable microbial communities in the trench-bound and wedge toe sediments and in considering the limits of their spatial distribution in this deep-sea sedimentary setting.

## **METHODS**

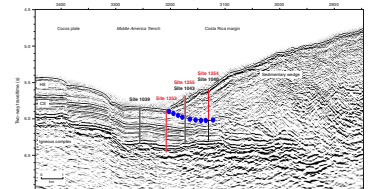
### **Sampling Protocol**

Leg 205 revisited Leg 170 sites for more focused study of the Costa Rica forearc. Sites 1039, 1043, and 1040, cored during Leg 170, correspond to Leg 205 Sites 1253, 1255, and 1254, respectively (see Fig. F2). Most of the cored depths were washed (i.e., no sediments were retrieved), and rotary core barrel (RCB) drilling was used to maximize rapid penetration to the depths of interest. These were not ideal drilling conditions for microbiological sampling, but special care was taken to obtain high-quality sediment samples. Samples collected for biomarker analyses are from the incoming carbonate section of Site 1253 at 370–437 mbsf, in the forearc sedimentary wedge décollement zone at Site 1255 at 134–145 mbsf, and around an upper fault (153–220 mbsf) and in the décollement zone (305–366 mbsf) at Site 1254 (Table T1). Throughout shipboard coring, 5-cm-long whole-round samples were selected for microbiological sampling adjacent to interstitial water whole rounds. Whole-round samples were transported to the shipboard microbiology laboratory for paring and sampling. Two plugs were extracted from cleaned sediment using autoclaved cut-off syringes and

**F1.** Regional bathymetry, p. 15.



**F2.** Seismic reflection profile, p. 16.



**T1.** Biomarker data, p. 23.

were expelled from the syringes immediately into sterile 15-mL plastic tubes, capped tightly, and frozen at  $-80^{\circ}\text{C}$  for postcruise DNA screening and microbial community assessment. Samples typically consisted of  $\sim 10$  g dry weight sediment, although some samples were as great as 20 g dry weight sediment. One whole-round sample (Sample 205-1255A-2R-2, 43–48 cm) consisted primarily of drilling slurry (i.e., a mixture of material from overlying sedimentary formations and seawater used to cool the bit during drilling) and was inappropriate for microbiological sampling; it was treated as all other samples for the purpose of characterizing cell and biomarker content of the drilling mud. Samples of drilling fluid running out of the core liner when first placed on the catwalk were obtained in 50-mL sterile plastic tubes. Prior to analysis, samples were lyophilized in preparation for serial extraction of DNA and lipids.

### **Laboratory Techniques**

As discussed in Peacock et al. (2004) and White et al. (1996), a modification of the Bligh and Dyer technique (Bligh and Dyer, 1954; Kehrmeier et al., 1996) was used to extract and fractionate biomarker compounds from the environmental sample. All sediment samples were freeze-dried, powdered with porcelain mortar and pestle, weighed, transferred to glass tubes (all tubes were cleaned, rinsed with deionized water, and heated to  $450^{\circ}\text{C}$  for 6 hr prior to use), and capped with acetone-rinsed polytetrafluoroethylene (PTFE)-lined tops. Phosphate buffer, methanol, and chloroform were added to samples, and after a period of shaking and centrifugation, the supernatant containing the total lipid (organic) fraction was separated. Nanopure water (extracted with chloroform) was added to the supernatant, the tubes were well shaken, and DNA was isolated in the aqueous phase. A silicic acid slurry was loaded onto fractionation columns, which were flushed with acetone and chloroform. Samples were then pipetted onto the silicic acid bed. Once the columns were loaded, 5 mL of *n*-hexane was applied as a purification step; the eluant was captured and dried under nitrogen. The column was then flushed with 5 mL of chloroform; the eluant containing neutral lipids was captured and dried under nitrogen. The column was flushed with 5 mL of acetone; the eluant containing glycolipids was captured and dried under nitrogen. The column was then flushed with 5 mL of methanol; the eluant containing polar lipids was captured and dried under nitrogen.

### **Contamination Assessment**

Procedural blanks were included in the protocol and analyzed with samples; no laboratory-related contamination of DNA or biomarker lipids was detected. Analysis of drilling fluid samples did not reveal DNA or PLFA in detectable amounts but did show some quinone content; the quinone types may not suggest sources in aerobic communities but may be inherited as fossils from either the sedimentary environment itself or from seawater entrained during core drilling or retrieval through the water column. Drilling slurry sampled in Sample 205-1255A-2R-2, 43–48 cm, showed a high ubiquinones/menaquinones (UQ/MK) ratio, reflecting input of cell material associated with aerobic respiration, which is discussed below in greater detail. Measures taken to pare intact biscuits of sediment from whole-round samples were thus necessary to successful elimination of contamination.

### **Ester-Linked Phospholipid Fatty Acid Analysis**

Analysis of PLFAs in the samples was carried out via capillary gas chromatography with mass spectrometry (GC-MS) in positive ion electron impact mode, as in Peacock et al. (2004). Detection limit is estimated at ~1 pmol, or  $10^4$  *Escherichia coli*-sized cells per gram extracted sediment. We are aware of the problems in PLFA measurement in low-biomass environments (see Tunlid et al., 1989).

### **DNA Fluorometry**

Cold isopropanol was used to precipitate nucleic acids out of the aqueous phase. SYBR green dye was then applied. The dye binds to double-stranded DNA, and fluorometry was used to screen for DNA. Hoechst dye was used in this technique, with a 10 ng/mL detection limit.

### **Methanogen Gene Copy Number Estimation**

Samples that contained DNA were subjected to subsequent screening for methanogens by real-time polymerase chain reaction (PCR), employing ME1 and ME2 primers that amplify a 0.75-kb region of the  $\alpha$ -subunit gene for methyl coenzyme M reductase (MCR), an enzyme that is essential for reactions necessary for methanogenesis. The detection limit of real-time PCR for methanogens is 100 cells/g solution (i.e., sediment extract). For quantitative data with an estimated uncertainty within 1%, the quantitation limit is 1000 cells/g solution. Data reported between 100 and 1000 cells/g solution are estimated values; these data exhibit real, relative differences in mcr gene copy numbers but have greater absolute uncertainty due to low signal intensity. For this study, samples that showed detectable levels of MCR genes range between ~200 and ~1300 cells/g solution. Real-time PCR amplification was performed using the protocol recommended by the manufacturer in an ABI 7000 sequence detection system (Applied Biosystems). Reaction mixtures (30  $\mu$ L) contained each deoxynucleoside triphosphate at a concentration of 200  $\mu$ M, each primer at a concentration of 2.5  $\mu$ M, 1 $\times$  cloned *Pyrococcus furiosus* (Pfu) polymerase buffer (Stratagene, La Jolla, California, USA), SYBR green (1:30000, Molecular Probes, Eugene, Oregon, USA), and 1U PfuTurbo HotStart DNA polymerase (Stratagene). Thermal cycle parameters were as follows: 10 min at 95°C, then 30 cycles of 60 s at 95°C, 60 s at 50°C, and 120 s at 75°C. A calibration curve was obtained by using a serial dilution of a known concentration of positive control DNA. The values obtained from each sample were then compared with the standard curve to determine the original sample DNA concentration. In a waste treatment facility, the percent of ammonia oxidizing bacteria represented 1.7% of the community based on the Q PCR of the essentially universally distributed amoA gene and 2.9% based on the 16S ribosomal DNA (rDNA) ammonia-oxidizing bacteria; this shows excellent agreement between the quantitative assessment of a functional gene and the phylogenetic 16S rDNA, which has been shown to correlate very well with many other cellular biomarkers (Harms et al., 2003).

### **Quinone Profiling**

Quinones in sedimentary neutral lipids were extracted in dim light. Liquid chromatography–mass spectrometry (LC-MS) of neutral lipid ex-

tract from sediment samples identified major quinones present, as detailed in Geyer et al. (2004). Briefly, neutral fractions were introduced to an MDS/Sciex API 365 tandem mass spectrometer by atmospheric pressure chemical ionization (APCI) source and analyzed in multiple reaction monitoring mode. In this method, the first quadrupole filtered each molecular species based on the mass/charge ( $m/z$ ) ratio of the corresponding quasimolecular ions and the second scanning quadrupole was set at  $m/z$  ratios 187 and 197 to find each compound class, menaquinone and ubiquinone, respectively. The method itself has a detection limit of 0.1 nmol/mL for each sample with 10- $\mu$ L injections, but the apparent limit of detection (LOD) was affected by preceding sample processing steps, including the extraction for preconcentration. This laboratory methodology results in higher sensitivity (or lower LOD) for larger amounts of processed sample; the range of LOD values that apply to the current study was 0.05–2 pmol quinones/g dry sediment, dependent on initial sample mass. Sample-specific detection limits (SSDL) are provided in Table T1. Quinone distribution is sensitive to the respiring strategies of microbes active now or in the past. With a change in terminal electron acceptor, a mixed bacterial drinking water biofilm greatly modified its content and ubiquinone/menaquinone ratio in 24 hr (Geyer et al., 2004). It may be, however, that fossil quinones are impacting present analytical results. Concentrations of quinones compared to those of PLFAs indicate that the former group contains a substantial fossil fraction.

## RESULTS

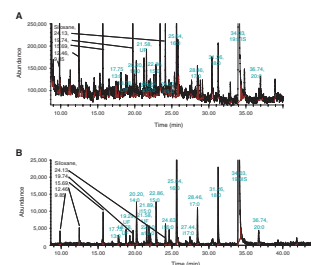
Summary biomarker data are presented in Table T1.

PLFAs were detected in 8 of the 26 samples, documenting viable eubacterial presence in those samples. Any Archaeal lipids in these samples would not impact the PLFA signal because Archaeal lipids are ether-linked and are not detectable using this technique. At wedge Site 1254, the maximum PLFA content was observed in the décollement interval. Elevated occurrence of hydrocarbons (up to 10 carbon atom chains, reported by Shipboard Scientific Party, 2003a) in gas and fluids sampled shipboard during Leg 205, imply significant deeply sourced fluid flux in that microenvironment. At reference Site 1253, PLFAs were detected in one sample from the base of the carbonate section only. At wedge Site 1255, the highest PLFA content of the entire sample set was found in the shallow sedimentary wedge. Figure F3 provides both a representative gas chromatogram for Sample 205-1254A-11R-5, 103–108 cm, at 326.1 mbsf and an associated ion chromatogram for  $m/z = 75$  to illustrate fatty acid methyl ester (FAME) distribution.

DNA was identified by fluorometry in 13 of 26 samples tested. Samples with DNA include carbonates from the incoming section, as well as forearc wedge sediments, spanning all three coring sites. There is no regular distribution of DNA with increasing depth or sedimentary structures, possibly because of the relatively high detection limit of the fluorometric method used. It is possible that fossil DNA could be present and complicating this signal (see Dell'Anno et al., 1998), although because DNA was not detected in every sample, we believe we are observing distinct habitable zones in the sediment column.

Methanogen-specific genes were detected in DNA extracted from one reference Site 1253 sample (at 436.9 mbsf in the basal carbonates) and

F3. Gas and ion chromatograms, p. 17.



four wedge Site 1254 samples (at 161.2 and 197.4 mbsf in the upper prism and at 326.1 and 330.3 mbsf in the décollement).

Quinone data (presented in Table T1) showed the most variation across samples, with measurable concentrations in every sample. Quinones are useful biomarkers because respiratory processes require specific quinones as electron shuttling components in cell membranes. Ubiquinones are found in eukaryotes and Gram-negative bacteria (reflecting growth with oxygen, or in some cases nitrate, as the terminal electron acceptor), and menaquinones are found in Archaea and Gram-positive bacteria and Gram-negative bacteria utilizing anaerobic terminal electron acceptors (Hedrick and White, 1986; Hiraishi, 1999). The problems with quinones as biomarkers of viable cells are that the rates of turnover of quinones outside the cells are unknown and the high levels relative to PLFA detected herein could represent quinone fossils. Inside living bacteria, respiratory quinones have a turnover measured in days, and in aerobically grown *E. coli*, the PLFAs have 100 times greater molar concentration than the ubiquinones (Geyer et al., 2004).

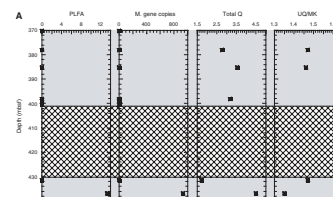
RCB cores require extensive paring of the whole-round sample to eliminate drilling contamination in microbiological samples, resulting in small final sample volumes. Contamination was largely prevented because (1) sediments were obtained from whole-round samples using the most meticulous, sterile sampling techniques possible, and (2) material was taken from intact sediment cores or pared biscuits in whole-round samples. One drilling slurry sample and three core fluid samples were not below detection in every analysis for cellular material employed here; therefore, the possibility of contamination with drilling-related material does exist. Such material would likely be inherited from shallower depths in the same drill hole or from surface seawater used as drilling fluid, making it more difficult to relate biomarker data to a specific depth in the sediment column. However, the rigorous sampling techniques used in this study, following conventional microbiological sampling protocols, and the cases where data show biomarker abundance greater than that in one slurry sample, convince us that the data provide real information about the deep subseafloor drilled during Leg 205.

## DISCUSSION

Clear evidence for viable microbial communities downhole exists, although biomarker abundances are low (Fig. F4). This is based on detection of PLFAs, which indicate intact cell membranes (Pinkart et al., 2002). Here we examine possible linkages between biomarker distribution and other aspects of the Costa Rica habitat before going on to a more detailed discussion of quinone and methanogen-specific gene copy number data.

Sediment geochemistry and mineralogy provide chemical and textural substrate for microbial activity. Mn and Fe are reactants in known metabolic reactions of marine sediment-hosted microbes and are metals involved in the production of bacterial enzymes, coenzymes, and cofactors. These and other metals have been mined by microbes from silicates under controlled and natural conditions (see Brantley et al., 2001; Rogers and Bennett, 2004; Thorseth et al., 2001). Bulk sediment data produced shipboard during Leg 205 on Site 1254 samples adjacent to those used for microbial assays show that these sediments contain 7.36–9.54 wt% Fe<sub>2</sub>O<sub>3</sub>, 0.04–0.10 wt% MnO, 57.8–106.0 ppm Cr, and

F4. PLFA, gene copy number, quinones, and UQ/MK ratio, p. 18.



74.1–82.3 ppm Cu (Shipboard Scientific Party, 2003c). Site 1255 data are similar. Site 1253 data reflect the carbonate lithology of the sediments, with 1.55–3.39 wt% Fe<sub>2</sub>O<sub>3</sub>, 0.14–0.38 wt% MnO, 20.7–45.0 ppm Cr, and no detectable Cu (Shipboard Scientific Party, 2003d). Although the oxidation states of Fe and Mn in this sedimentary setting are not known, metal content appears sufficient for microbial activity.

Core descriptions and X-ray diffraction data on bulk sediment samples (Shipboard Scientific Party, 2003c, 2003d) indicate that the Site 1254 and 1255 wedge sediments are dominantly clay and the Site 1253 basal carbonates are a fairly clean calcareous ooze (Shipboard Scientific Party, 2003b). Clay minerals may trap organic compounds by adsorbing them to charged clay surfaces or preserving them in interlayer spaces (Moore and Reynolds, 1997). The high clay content of the wedge sediments may then control their organic carbon load and create suitable habitat for microbes. Carbonates at Site 1253 are not clay rich, but alteration processes have left a relatively metal rich imprint on the basal carbonates, which may enhance their habitability (Shipboard Scientific Party, 2003b) and could lead to the observed presence of methanogen-specific gene copies, PLFAs, and quinones documented here (Fig. F3).

There is a suggestion in the data that increases in total quinone content, a proxy for total biomass (Hiraishi, 1999), are associated with fluid flow from deeper in the subduction zone along the décollement (Fig. F4B). It may be that on the scale of interstitial pore space volumes, accessibility of biologically necessary elements is important; grain textures and degree of alteration of mineral surfaces may help or hinder microbial processing of these important metals from the solid phase, and the fluid-borne component becomes crucial to community survival. The heterogeneity of this system is considerable, and the irregular nature of the biomarker distribution is not unexpected. In the future, greater sampling density in areas of known high fluid flow will provide critical data to evaluate this hypothesis further, as will the full spectrum of chemical analyses possible in the large-volume osmotically sampled fluids recovered during IODP Expedition 301T (Kastner et al., 2004).

Although PLFA data do indicate the presence of intact cell membrane components at certain sampled intervals (Table T2; Fig. F4), quinones were detected across all samples and are thus a very useful means of comparison. Indexes of quinone variation express aspects of the quinone data set for these samples. Ubiquinones are abbreviated as UQ (used in aerobic respiration of Gram-negative bacteria and microeukaryotes), menaquinones as MK (used in Archaea and Gram-positive bacteria and for anaerobic respiration in Gram-negative bacteria), plastoquinones as PQ (necessary for energy conversion in photosynthesis), and phylloquinones as K<sub>1</sub> (product of photosynthesis). As in Hirashi et al. (1999), the microbial divergence index is

$$MD_q = \left( \sum_{k=1}^p \sqrt{x_k} \right)^2$$

where  $x_k \geq 0.001$  and indicates the molar ratio of quinone ( $k$ ) to total quinone content, normalized to unity, and the bioenergetic divergence index is

$$BD_q = [\sqrt{UQ} + \sqrt{(PQ + K_1)} + \sqrt{MK}]^2$$

where UQ, (PQ + K<sub>1</sub>), MK  $\geq 0.001$ , and UQ, PQ, K<sub>1</sub>, and MK are the molar fractions of those quinones compared to total quinone content.

---

T2. PLFA data, p. 24.

---



Note that  $MD_q$  manipulates all quinones in the same fashion, but  $BD_q$  splits quinones into respiratory classes. Table T3 provides numerical data for these microbial diversity indexes. Essentially,  $MD_q$  reflects the diversity of respiratory quinones encountered in a sample, whereas  $BD_q$  reflects the mode of respiration that dominates in a sample. All samples tracked in this study reflect dominantly anaerobic respiratory pathways, with no evidence of PQ or  $K_1$ , and therefore no role for photosynthesis in these communities, and low relative abundances of aerobically utilized UQ. As we stated earlier, respiratory quinones are biological products but we cannot establish their relationship to the currently viable microbiota reflected in the PLFAs, as the turnover in these or other possible extracellular environments have never been determined.

Site 1254 microbial diversity indexes (Fig. F5A, F5B) illustrate that there is or has been observable change in community structure downcore. Data for samples above 197 mbsf indicate a fairly stable, somewhat diverse community presence now or in the past (upper black circles; boxed in Fig. F5B), with similar proportions of UQ and MK. Community structure changes at the base of the upper fault zone (blue squares; samples at ~200–220 mbsf), shifting to a less diverse community with UQ and MK present in different proportions. Deeper in the sedimentary strata, data show some scatter in the décollement zone (green triangles; ~340–364 mbsf) and incremental gains in both index values as the décollement is approaching. This suggests that from ~306 to ~330 mbsf there is or has been a horizon with more variable microbial quinones. Figure F5B highlights differences in the downhole microbial community at Site 1254. Interestingly, Site 1254 samples from within the upper prism fault (blue squares) and the décollement (green triangles) are the samples that span nearly the entire range of  $BD_q$  for this site, yet have lower  $MD_q$  values than the samples above 197 mbsf.

To generate a concise representation of the variation in the quinone data set, principal component analysis (PCA) was carried out on the correlation matrix of quinone values; this statistical analysis (carried out in JMP version 5.1 [JMP The Statistical Discovery Software, [www.jmp.com](http://www.jmp.com)]) reduces the dimensionality of the original data set, representing data for all 11 quinones in two-dimensional space. PCA provides composite variables to portray the overall variability across samples in a concise way, showing here that MK4 and MK5 distinguish sample groups across all samples considered from Sites 1253, 1254, and 1255 (Table T4) and also at Site 1254 alone (Table T4); principal components 1 (PC1) and 2 (PC2) explain ~96% of the variation in both cases. PC1 loads on all quinones, shown by near-equivalent eigenvector values, are likely controlled by biomass levels in sediment. PC2 loads heavily on MK4 and MK5, shown by eigenvector elements of greater magnitude for MK4 and MK5 than for other quinones. Ubiquinones are found in Gram-negative *Proteobacteria*, some purple photosynthetic bacteria growing anaerobically, and a few *Actinobacteria*, most of which have MKs. Recently, large amounts of UQ-8 have been found in the anaerobe *Dehalococcoides* (White et al., 2005).

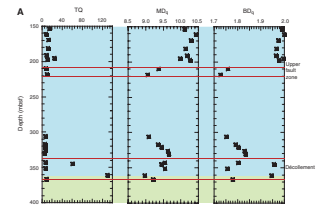
MK4 and MK5 are menaquinones broadly associated with anaerobic respiratory strategies in Gram-negative eubacteria and Gram-positive eubacteria. These quinones are common to large groups of Archaea and Bacteria (Hiraishi, 1999), though studies relating MK4 and MK5 to specific links in metabolic pathways do not yet exist. Ongoing work on the taxonomic significance of quinone types may provide novel perspectives on these data over time. At present, the impact of MK4 and MK5 on downhole community structure is not clear.

---

T3. Quinone indexes, p. 25.

---

F5. Downhole variation in TQ,  $MD_q$ , and  $BD_q$ , p. 21.



---

T4. Eigenvalues and eigenvectors, p. 26.

---

The documented movement of fluids through this forearc environment (McAdoo et al., 1996) maintains chemical disequilibrium, and likely generates habitable zones throughout, by flushing sediment pore spaces with hydrocarbon-bearing fluids with metal chemistries different from ambient interstitial water. Chemosynthetic microbial communities in this deep seafloor environment depend on sources of carbon and energy for survival. Carbon is available as residual organic carbon in the sedimentary strata and in gas-phase hydrocarbons, particularly methane, in the pore spaces. Energy can be gleaned from any number of redox couples available in the system:  $\text{SO}_4^{2-}/\text{S}^{2-}$ , Fe(III)/Fe(II), and Mn(IV)/Mn(II), among others. Sediment-hosted total organic carbon constitutes ~0.5–2.1 wt% of the bulk sediment (Shipboard Scientific Party, 1997a, 1997b), providing raw material for reactions producing biogenic methane in situ and eventually thermogenic hydrocarbons as residual carbon subducts to hotter, deeper environments. Increasing overburden and tectonic compression at convergent margins causes compaction dewatering of subducted sediment. At Costa Rica, a considerable flux of thermogenic hydrocarbons (up to hexane, as reported in Shipboard Scientific Party, 1997b) to the hydrosphere is observed, via fault networks and diffuse seepage to the seafloor. These thermogenic hydrocarbons arise from thermal decomposition of organic matter in the deeper subduction zone, and combined with fluid advection they may fuel seafloor methanotrophy (as described in Hinrichs et al., 2000; Mills et al., 2003).

Hydrocarbons associated with the sediments sampled offshore Costa Rica bear a mixture of both deeply sourced, thermogenic hydrocarbons (including methane, ethane, and propane) and also isotopically light biogenic hydrocarbons ( $\delta^{13}\text{C}$   $\text{CH}_4$  is approximately  $-80\text{‰}$ ;  $\delta^{13}\text{C}$   $\text{C}_2\text{H}_6$  is approximately  $-55\text{‰}$ ) (Lückge et al., 2002) produced in the shallower seafloor. The microbially generated “biogenic” methane, likely produced from reworked thermogenic methane and other hydrocarbons and/or refractory organic compound precursors, dominates the methane in the sedimentary system (Lückge et al., 2002).

In the present study, the prospect of identifying explicit variation in microbial communities in the Costa Rica convergent margin forearc, rather than inferring it from, for example, interstitial water geochemistry and/or stable isotope systematics of methane, is a compelling one. From the biomarker data presented above, we infer possible variation in respiratory strategies with depth in the Costa Rica sedimentary wedge (Site 1254) and basal carbonates (Site 1253) at some time prior to sampling. The regular variation in indexes of microbial diversity and bioenergetics above the décollement at Site 1254 (described above) suggests that some aspect of that sedimentary habitat, such as sediment texture or enrichment in deeply sourced fluids, exerted real control on the past or present microbial community.

## **CONCLUSIONS**

This is the first analysis of microbial community structure in the deep subsurface near the Costa Rica Trench and one of few studies focused on the deep biosphere associated with convergent margins. Based on DNA detection, methanogen-specific gene detection, PLFA presence, and quinone profiles, we show that microbial communities exist/existed in the seafloor sediments. Furthermore, we document that within the décollement and sedimentary wedge fault zone, both sites of

deeply sourced hydrocarbon-bearing and chemically distinct fluid flow, microbial diversity and bioenergetic strategies differ from those of background sediment.

## **ACKNOWLEDGMENTS**

This research used samples and data provided by the Ocean Drilling Program (ODP). ODP is sponsored by the U.S. National Science Foundation (NSF) and participating countries under management of Joint Oceanographic Institutions (JOI), Inc. Funding for this research was provided by the U.S. Science Support Program. In particular, we recognize Dr. Sung-Chan Jo, Chromatography/Mass spectrometry Lab Coordinator at the Center for Biomarker Analysis (Knoxville, Tennessee, USA) for his attention to high-quality data generation. Amanda Smithgall and members of the research team at Microbial Insights (Knoxville, Tennessee, USA) are also thanked for their analytical assistance. We are grateful to Kai-Uwe Hinrichs, Klaus-G. Zink, and the ODP editorial staff for their insightful and comprehensive review comments, which significantly improved the manuscript.

## REFERENCES

- Biddle, J.F., Lipp, J.S., Lever, M.A., Lloyd, K.G., Sørensen, K.B., Anderson, R., Fredricks, H.F., Elvert, M., Kelly, T.J., Schrag, D.P., Sogin, M.L., Brenchley, J.E., Teske, A., House, C.H., and Hinrichs, K.-U., 2006. Heterotrophic archaea dominate sedimentary subsurface ecosystems off Peru. *Proc. Natl. Acad. Sci. U. S. A.*, 103(10):3846–3851. doi:10.1073/pnas.0600035103
- Bligh, E.G., and Dyer, W.J., 1954. A rapid method of total lipid extraction and purification. *Can. J. Biochem. Physiol.*, 37:911–917.
- Brantley, S.L., Liermann, L., Bau, M., and Wu, S., 2001. Uptake of trace metals and rare earth elements from hornblende by a soil bacterium. *Geomicrobiol. J.*, 18(1):37–61. doi:10.1080/01490450151079770
- Dell'Anno, A., Fabiano, M., Duinefeld, G.C.A., Kok, A., and Danovaro, R., 1998. Nucleic acid (DNA, RNA) quantification and RNA/DNA determination in marine sediments: comparison of spectrophotometric, fluorometric, and high-performance liquid chromatography methods and estimation of detrital DNA. *Appl. Environ. Microbiol.*, 64:3238–3245.
- DeMets, C., Gordon, R.G., Argus, D.F., and Stein, S., 1990. Current plate motions. *Geophys. J. Internat.*, 101:425–478.
- D'Hondt, S., Jørgensen, B.B., Miller, D.J., Batzke, A., Blake, R., Cragg, B.A., Cypionka, H., Dickens, G.R., Ferdelman, T., Hinrichs, K.-U., Holm, N.G., Mitterer, R., Spivack, A., Wang, G., Bekins, B., Engelen, B., Ford, K., Gettemy, G., Rutherford, S.D., Sass, H., Skilbeck, C.G., Aiello, I.W., Guèrin, G., House, C.H., Inagaki, F., Meister, P., Naehr, T., Niitsuma, S., Parkes, R.J., Schippers, A., Smith, D.C., Teske, A., Wiegel, J., Naranjo Padilla, C., and Acosta, J.L.S., 2004. Distributions of microbial activities in deep seafloor sediments. *Science*, 306(5705):2216–2221. doi:10.1126/science.1101155
- Geyer, R., Peacock, A.D., White, D.C., Lytle, C., and Van Berkel, G.J., 2004. Atmospheric pressure chemical ionization and atmospheric pressure photoionization for simultaneous mass spectrometric analysis of microbial respiratory ubiquinones and menaquinones. *J. Mass Spectrom.*, 39(8):922–929. doi:10.1002/jms.670
- Harms, G., Layton, A.C., Dionisi, H.M., Gregory, I.R., Garrett, V.M., Hawkins, S.A., Robinson, K.G., and Sayler, G.S., 2003. Real-time PCR quantification of nitrifying bacteria in a municipal wastewater treatment plant. *Environ. Sci. Technol.*, 37(2):343–351. doi:10.1021/es0257164
- Hedrick, D.B., and White, D.C., 1986. Microbial respiratory quinones in the environment, I. A sensitive liquid chromatographic method. *J. Microbiol. Methods*, 5(5–6):243–254. doi:10.1016/0167-7012(86)90049-7
- Hinrichs, K.-U., Summons, R.E., Orphan, V., Sylva, S.P., and Hayes, J.M., 2000. Molecular and isotopic analysis of anaerobic methane-oxidizing communities in marine sediments. *Org. Geochem.*, 31(12):1685–1701. doi:10.1016/S0146-6380(00)00106-6
- Hiraishi, A., 1999. Isoprenoid quinones as biomarkers of microbial populations in the environment. *J. Biosci. Bioeng.*, 88(5):449–460. doi:10.1016/S1389-1723(00)87658-6
- Hiraishi, A., Umezawa, T., Yamamoto, H., Kato, K., and Maki, Y., 1999. Changes in quinone profiles of hot spring microbial mats with a thermal gradient. *Appl. Environ. Microbiol.*, 65(1):198–205.
- Kastner, M., Malone, M.J., and the Expedition 301T Project Team, 2004. Costa Rica hydrogeology. *IODP Sci. Prosp.*, 301T. doi:10.2204/iodp.sp.301T.2004
- Kehrmeyer, S.R., Applegate, B.M., Pinkart, H.C., Hedrick, D.B., White, D.C., and Sayler, G.S., 1996. Combined lipid/DNA extraction method for environmental samples. *J. Microbiol. Methods*, 25(2):153–163. doi:10.1016/0167-7012(95)00094-1
- Lückge, A., Kastner, M., Littke, R., and Cramer, B., 2002. Hydrocarbon gas in the Costa Rica subduction zone: primary composition and post-genetic alteration. *Org. Geochem.*, 33(8):933–943. doi:10.1016/S0146-6380(02)00063-3

- Mau, S., Sahling, H., Rehder, G., Suess, E., Linke, P., and Soeding, E., 2006. Estimates of methane output from mud extrusions at the erosive convergent margin off Costa Rica. *Mar. Geol.*, 225(1–4):129–144. doi:10.1016/j.margeo.2005.09.007
- McAdoo, B.G., Orange, D.L., Silver, E.A., McIntosh, K., Abott, L., Galewsky, J., Kahn, L., and Protti, M., 1996. Seafloor structural observations, Costa Rica accretionary prism. *Geophys. Res. Lett.*, 23(8):883–886. doi:10.1029/96GL00731
- Mills, H.J., Hodges, C., Wilson, K., MacDonald, I.R., and Sobecky, P.A., 2003. Microbial diversity in sediments associated with surface-breaching gas hydrate mounds in the Gulf of Mexico. *FEMS Microbiol. Ecol.*, 46(1):39–52. doi:10.1016/S0168-6496(03)00191-0
- Moore, D.M., and Reynolds, R.C., 1997. *X-Ray Diffraction and the Identification and Analysis of Clay Minerals* (2nd ed.): Oxford (Oxford Univ. Press).
- Newberry, C.J., Webster, G., Cragg, B.A., Parkes, R.J., Weightman, A.J., and Fry, J.C., 2004. Diversity of prokaryotes and methanogenesis in deep subsurface sediments from the Nankai Trough, Ocean Drilling Program Leg 190. *Environ. Microbiol.*, 6(3):274–287. doi:10.1111/j.1462-2920.2004.00568.x
- Parkes, R.J., Cragg, B.A., and Wellsbury, P., 2000. Recent studies on bacterial populations and processes in seafloor sediments: a review. *Hydrogeol. J.*, 8(1):11–28. doi:10.1007/PL00010971
- Parkes, R.J., Webster, G., Cragg, B.A., Weightman, A.J., Newberry, C.J., Ferdelman, T.G., Kallmeyer, J., Jørgensen, B.B., Aiello, I.W., and Fry, J.C., 2005. Deep sub-seafloor prokaryotes stimulated at interfaces over geological time. *Nature (London, U. K.)*, 436(7049):390–394. doi:10.1038/nature03796
- Peacock, A.D., Chang, Y.-J., Istok, J.D., Krumholz, L., Geyer, R., Kinsall, B., Watson, D., Sublette, K.L., and White, D.C., 2004. Utilization of microbial biofilms as monitors of bioremediation. *Microbiol. Ecol.*, 47(3):284–292. doi:10.1007/s00248-003-1024-9
- Pinkart, H.C., Ringelberg, D.B., Piceno, Y.M., Macnaughton, S.J., and White, D.C., 2002. Biochemical approaches to biomass measurements and community structure analysis. In Stahl, D.E., Hurst, C.H., Knudsen, G.R., McInerney, M.J., Stetzenbach, L.D., and Walter, M.V. (Eds.), *Manual of Environmental Microbiology* (2nd ed.): Washington (Am. Soc. Microbiol. Press), 101–113.
- Rogers, J.R., and Bennett, P.C., 2004. Mineral stimulation of subsurface microorganisms: release of limiting nutrients from silicates. *Chem. Geol.*, 203(1–2):91–108. doi:10.1016/j.chemgeo.2003.09.001
- Schippers, A., Neretin, L.N., Kallmeyer, J., Ferdelman, T.G., Cragg, B.A., Parkes, R.J., and Jørgensen, B.B., 2005. Prokaryotic cells of the deep sub-seafloor biosphere identified as living bacteria. *Nature (London, U. K.)*, 433(7028):861–864. doi:10.1038/nature03302
- Schmidt, M., Hensen, C., Mörz, T., Müller, C., Grevenmeyer, I., Wallmann, K., Mau, S., and Kaul, N., 2005. Methane hydrate accumulation in “Mound 11” mud volcano, Costa Rica forearc. *Mar. Geol.*, 216(1–2):83–100. doi:10.1016/j.margeo.2005.01.001
- Shipboard Scientific Party, 1997a. Site 1039. In Kimura, G., Silver, E., Blum, P., et al., *Proc. ODP, Init. Repts.*, 170: College Station, TX (Ocean Drilling Program), 45–93. [PDF]
- Shipboard Scientific Party, 1997b. Site 1040. In Kimura, G., Silver, E., Blum, P., et al., *Proc. ODP, Init. Repts.*, 170: College Station, TX (Ocean Drilling Program), 95–152. [PDF]
- Shipboard Scientific Party, 2003a. Leg 205 summary. In Morris, J.D., Villinger, H.W., Klaus, A., *Proc. ODP, Init. Repts.*, 205: College Station TX (Ocean Drilling Program), 1–75. [HTML]
- Shipboard Scientific Party, 2003b. Site 1253. In Morris, J.D., Villinger, H.W., Klaus, A., *Proc. ODP, Init. Repts.*, 205, 1–184 [CD-ROM]. Available from: Ocean Drilling Program, Texas A&M University, College Station TX 77845-9547, USA. [HTML]

- Shipboard Scientific Party, 2003c. Site 1254. In Morris, J.D., Villinger, H.W., Klaus, A., *Proc. ODP, Init. Repts.*, 205, 1–113 [CD-ROM]. Available from: Ocean Drilling Program, Texas A&M University, College Station TX 77845-9547, USA. [HTML]
- Shipboard Scientific Party, 2003d. Site 1255. In Morris, J.D., Villinger, H.W., Klaus, A., *Proc. ODP, Init. Repts.*, 205, 1–55 [CD-ROM]. Available from: Ocean Drilling Program, Texas A&M University, College Station TX 77845-9547, USA. [HTML]
- Takai, K., Moyer, C.L., Miyazaki, M., Nogi, Y., Hirayama, H., Nealson, K.H., and Hori-koshi, K., 2005. *Marinobacter alkaliphilus* sp. nov., a novel alkaliphilic bacterium isolated from subseafloor alkaline serpentine mud from Ocean Drilling Program Site 1200 at South Chamorro Seamount, Mariana forearc. *Extremophiles*, 9(1):17–27. doi:10.1007/s00792-004-0416-1
- Thorseth, I.H., Torsvik, T., Torsvik, V., Daae, F.L., Pedersen, R.B., and the Keldysh-98 Scientific Party, 2001. Diversity of life in ocean floor basalt. *Earth Planet. Sci. Lett.*, 194(1–2):31–37. doi:10.1016/S0012-821X(01)00537-4
- Toffin, L., Webster, G., Weightman, A.J., Fry, J.C., and Prieur, D., 2004. Molecular monitoring of culturable bacteria from deep sea sediment of the Nankai Trough, Leg 190 Ocean Drilling Program. *FEMS Microbiol. Ecol.*, 48(3):357–367. doi:10.1016/j.femsec.2004.02.009
- Tunlid, A., Ringelberg, D., Phelps, T.J., Low, C., and White, D.C., 1989. Measurement of phospholipid fatty acids at picomolar concentrations in biofilms and deep sub-surface sediments using gas chromatography and chemical ionization mass spec-trometry. *J. Microbiol. Methods*, 10(2):139–153. doi:10.1016/0167-7012(89)90010-9
- White, D.C., Geyer, R., Peacock, A.D., Hedrick, D.B., Koenigsberg, S.S., Sung, Y., He, J., and Löffler, F.E., 2005. Phospholipid furan fatty acids and ubiquinone-8: lipid biomarkers that may protect *Dehalococcoides* strains from free radicals. *Appl. Envi-ron. Microbiol.*, 71(12):8426–433. doi:10.1128/AEM.71.12.8426-8433.2005
- White, D.C., Stair, J.O., and Ringelberg, D.B., 1996. Quantitative comparisons of in situ microbial biodiversity by signature biomarker analysis. *J. Ind. Microbiol. Bio-techn.*, 17(3–4):185–196. doi:10.1007/BF01574692
- Whitman, W.B., Coleman, D.C., and Wiebe, W.J., 1998. Prokaryotes: the unseen majority. *Proc. Natl. Acad. Sci. U. S. A.*, 95(12):6578–6583. doi:10.1073/pnas.95.12.6578

Figure F1. Regional bathymetry offshore of the Nicoya Peninsula, Costa Rica, Central America. White box = Leg 205 and 170 drilling area (Shipboard Scientific Party, 2003a). Numbers 1–5 indicate depth in kilometers.

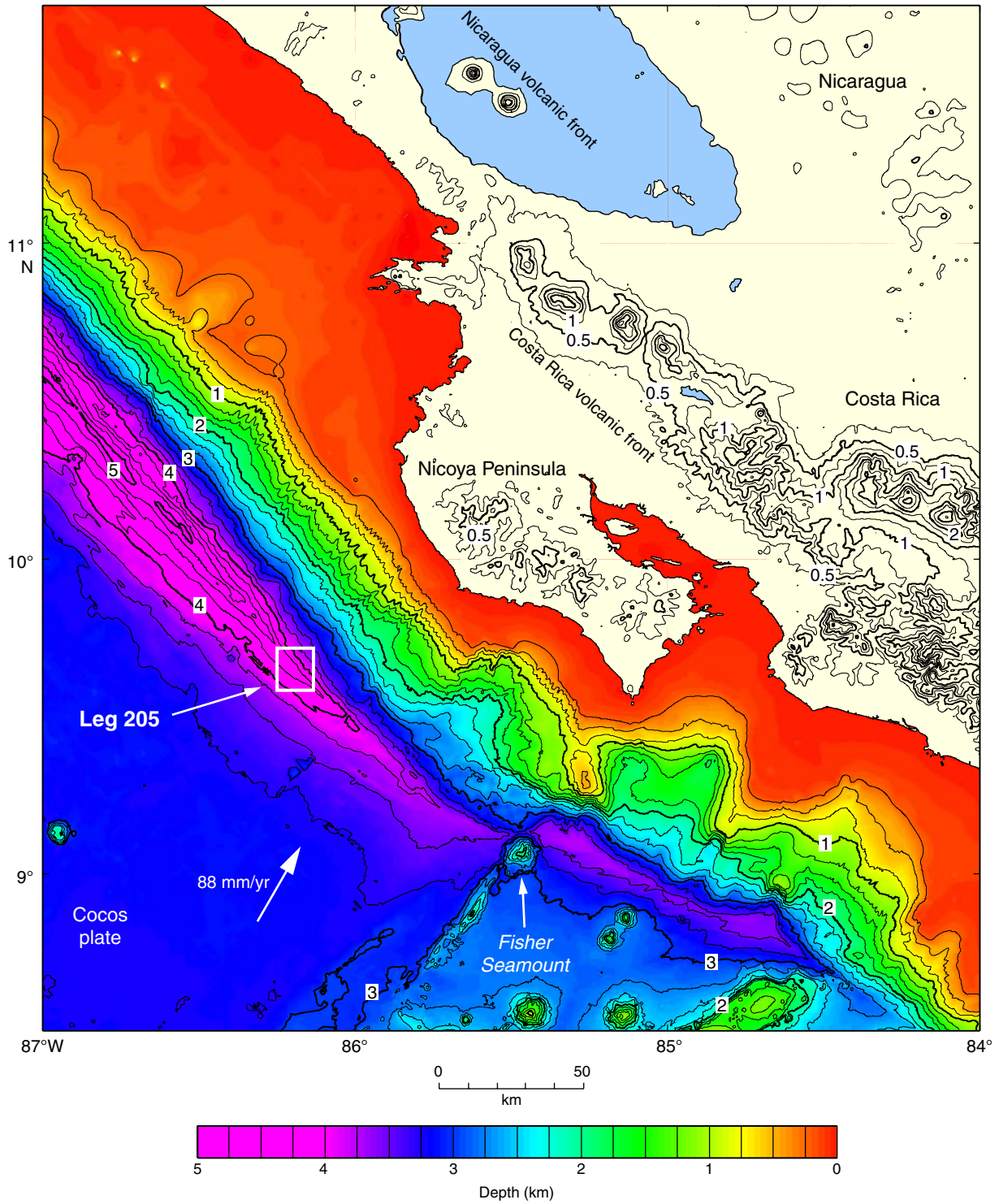


**Figure F2.** Seismic reflection profile across drilled sites in and near the Costa Rica sedimentary wedge. Black vertical lines show Leg 170 sites, red vertical lines show Leg 205 sites. Blue symbols approximate the décollement zone location. CMP = common midpoint, HS = hemipelagic sediments, CS = carbonate sediments (from Shipboard Scientific Party, 2003a).

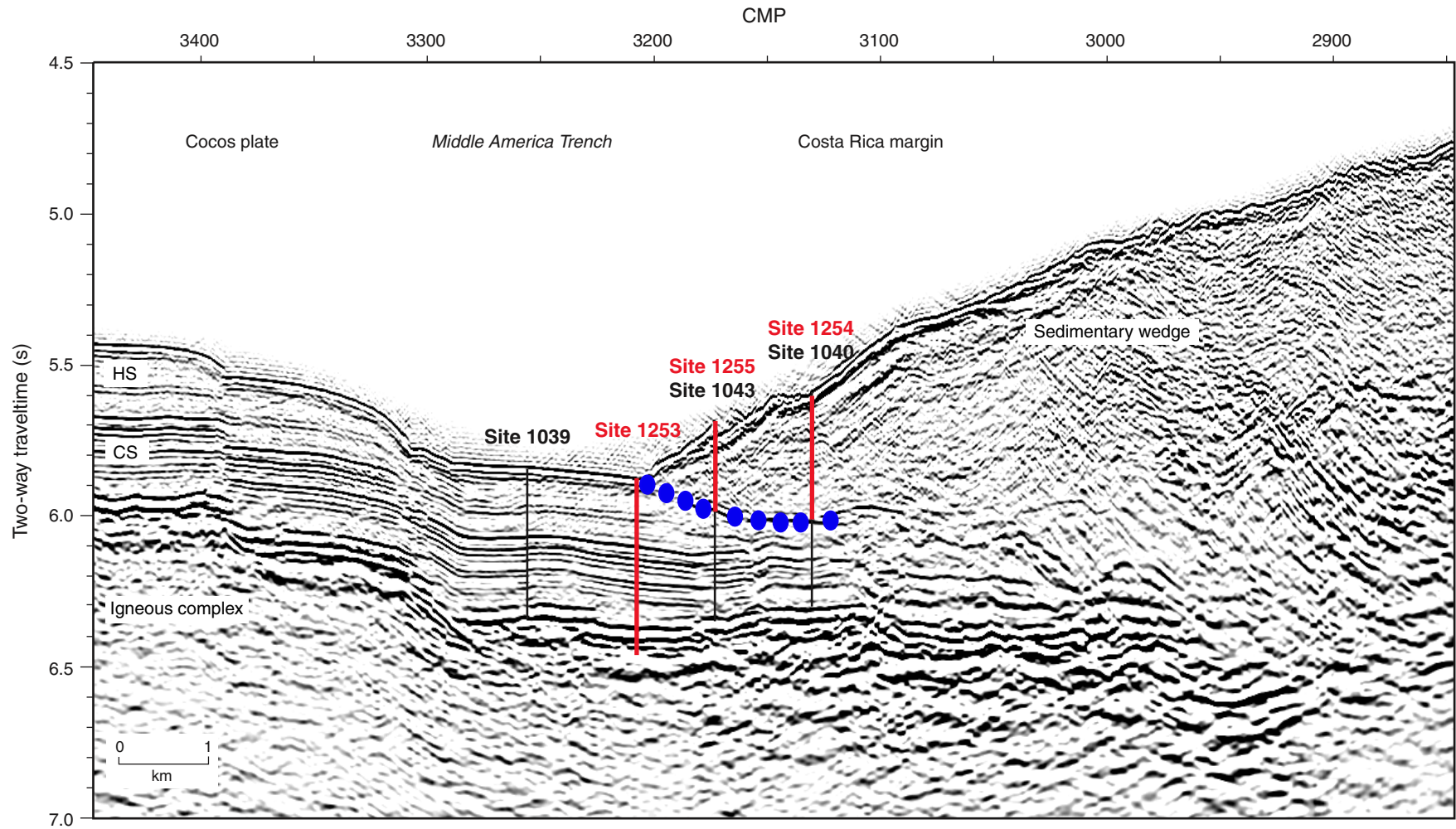




**Figure F3. A.** Representative gas chromatogram for PLFA analyses (Sample 205-1254A-11R-5, 103–108 cm; 326.1 mbsf). Dominant PLFA peaks for this sample include 14:0 (tetradecanoic acid, retention time = 20.20),  $\alpha$ 15:0 (anteiso branching pentadecanoic acid, retention time = 22.10), 15:0 (pentadecanoic acid, retention time = 22.86), 16:0 (hexadecanoic acid, retention time = 25.64), 17:0 (heptadecanoic acid, retention time = 28.46), and 18:0 (octadecanoic acid, retention time = 31.26). The presence of these PLFAs indicates the presence Gram-positive bacteria. **B.** Ion chromatogram of  $m/z$  74 (Sample 205-1254A-11R-5, 103–108 cm), labeled for FAME and other constituents. Unknown FAMES are labeled as “UF,” and peaks related to siloxane contamination are also indicated. IS = internal standard.

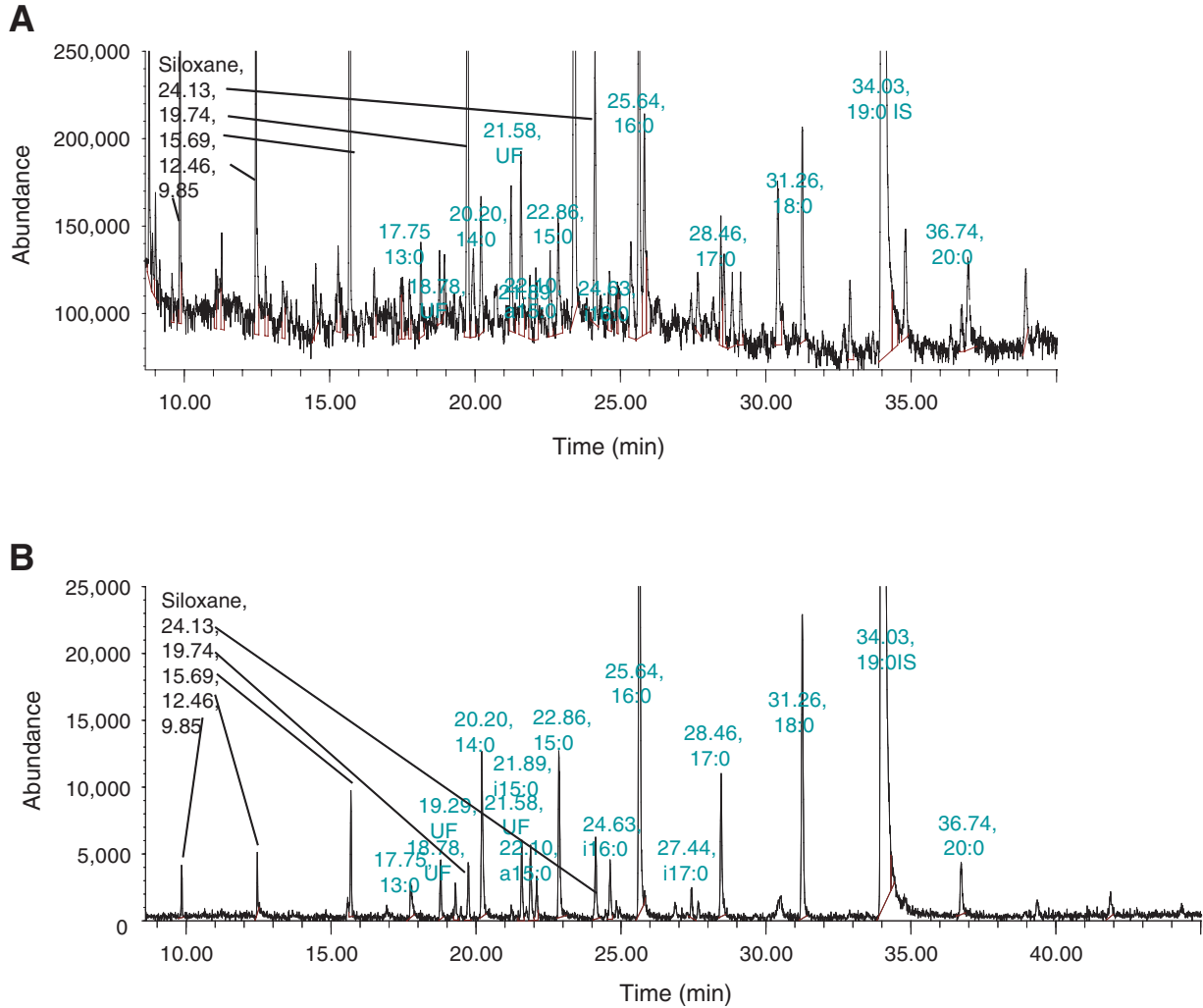


Figure F4. Total PLFA abundance, methanogen-specific (M.) gene copy number, total quinones (Q), and ubiquinone/menaquinone (UQ/MK) ratio data. A. Site 1253. Gray = lithologic Unit U3, an early to middle Miocene calcareous ooze with diatomaceous ooze and breccia; crosshatched area = intervening depths occupied by a gabbro sill (lithologic Subunit 4A) (Shipboard Scientific Party, 1997a). (Continued on next two pages.)

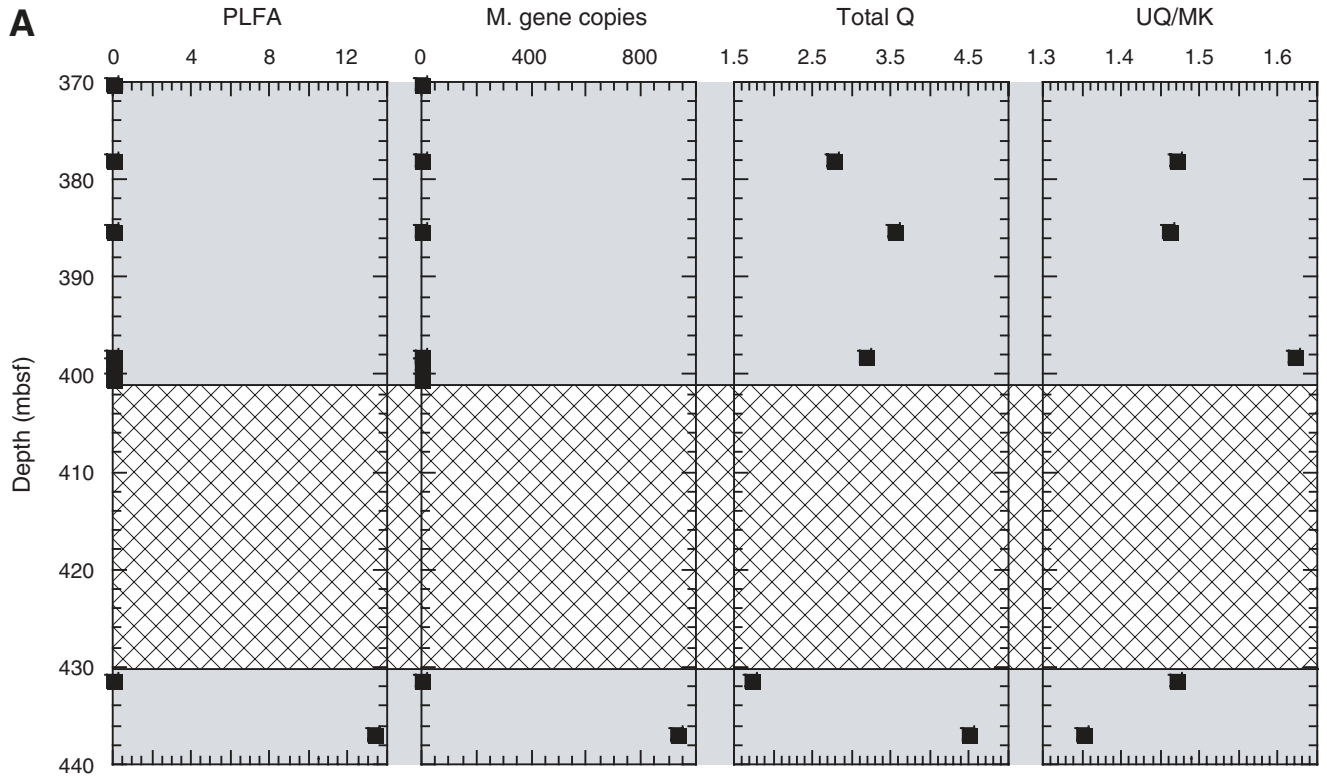


Figure F4 (continued). B. Site 1254. Blue = lithologic Unit P1B, a Pliocene–Pleistocene silty clay with silty or fine sand intervals, green = Unit U1, a clayey diatomite with silty sand interbeds (<0.20 Ma) (Shipboard Scientific Party, 1997b). Red lines = prism fault zone boundaries, with most concentrated shear between ~210 and 219 mbsf. Red lines = décollement boundaries at ~338.5 and ~364.2 mbsf (fault horizon depths from Shipboard Scientific Party, 2003a).

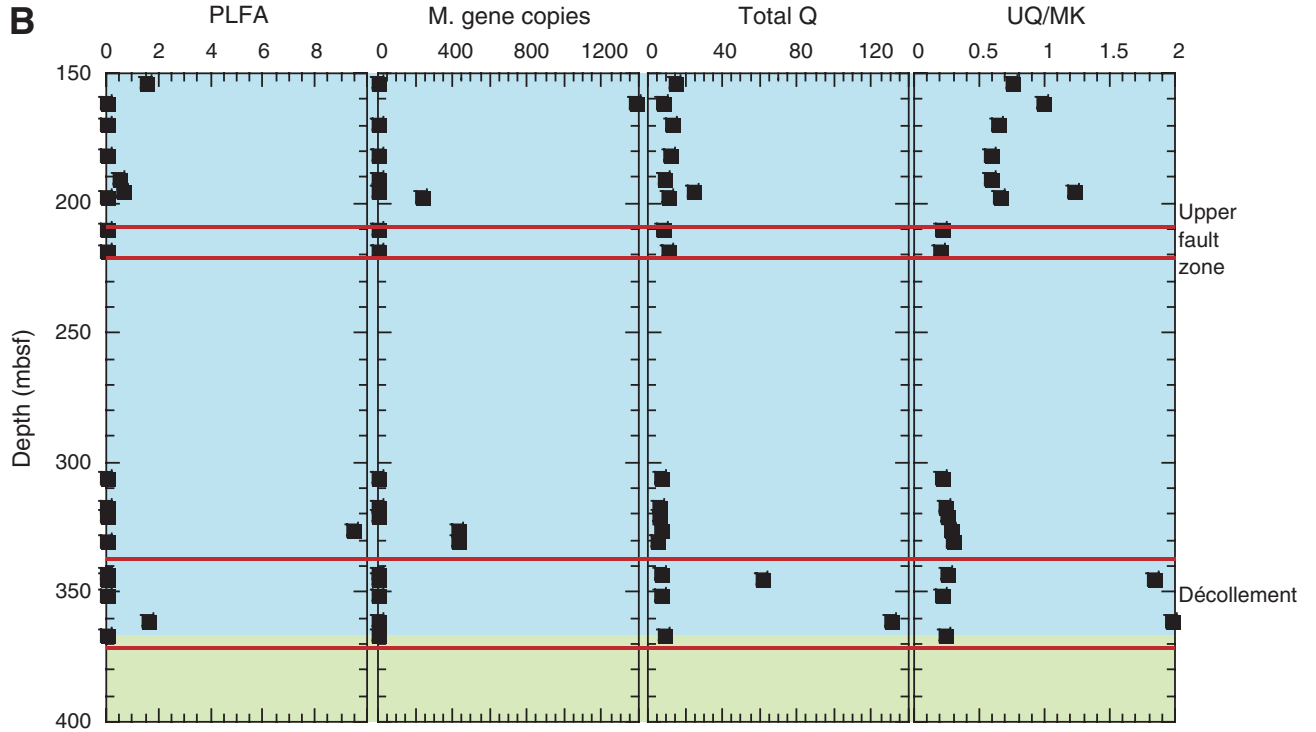


Figure F4 (continued). C. Site 1255. Methanogen-specific gene copy number data were below detection and are not plotted here. Blue = lithologic Unit T1 (for wedge toe sediments), which is equivalent to Unit P1B at Site1254; green = Subunit U1A, the topmost underthrust sediment. The base of the décollement and lithologic boundary coincide at ~144 mbsf (Shipboard Scientific Party, 2003a).

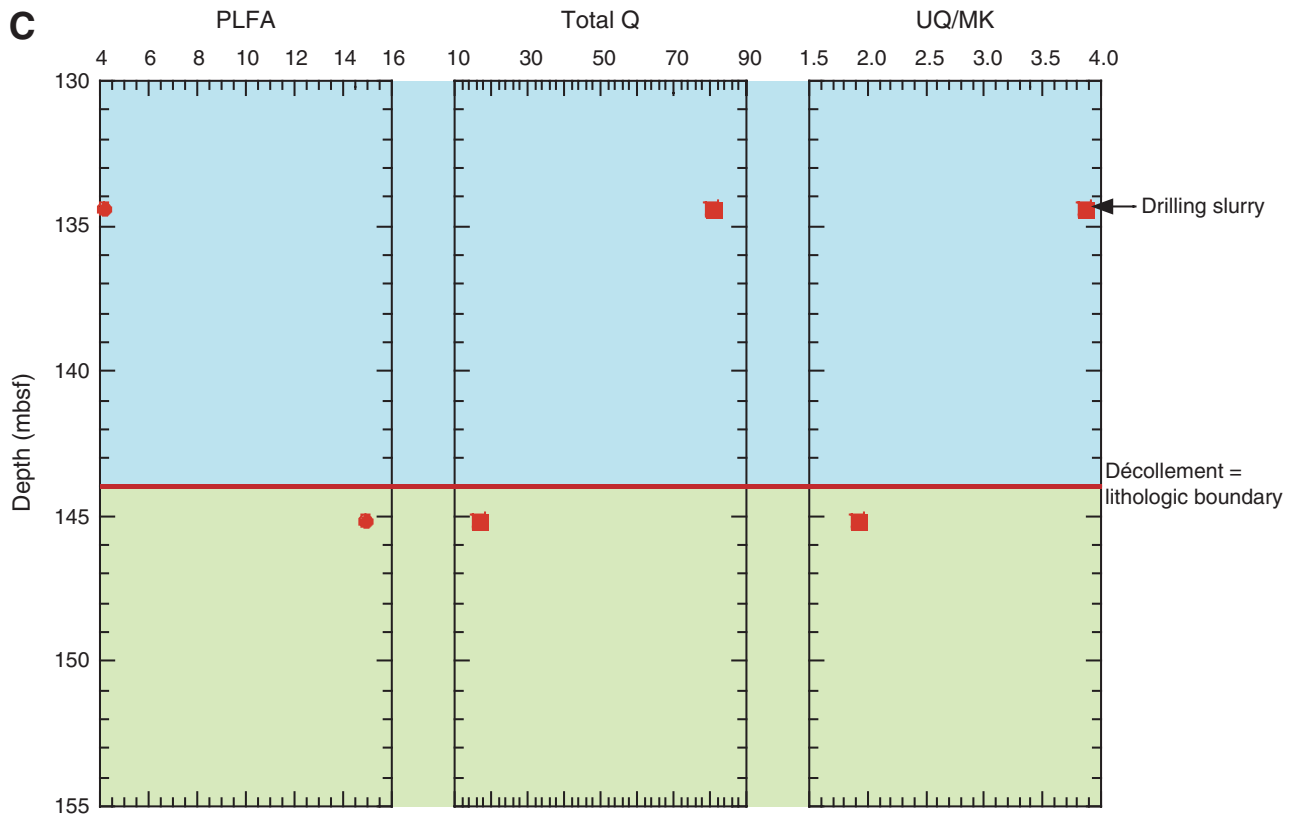


Figure F5. A. Downhole variation in total quinones (TQ), microbial divergence index ( $MD_q$ ), and bioenergetic divergence index ( $BD_q$ ) for Site 1254 samples. (Continued on next page.)

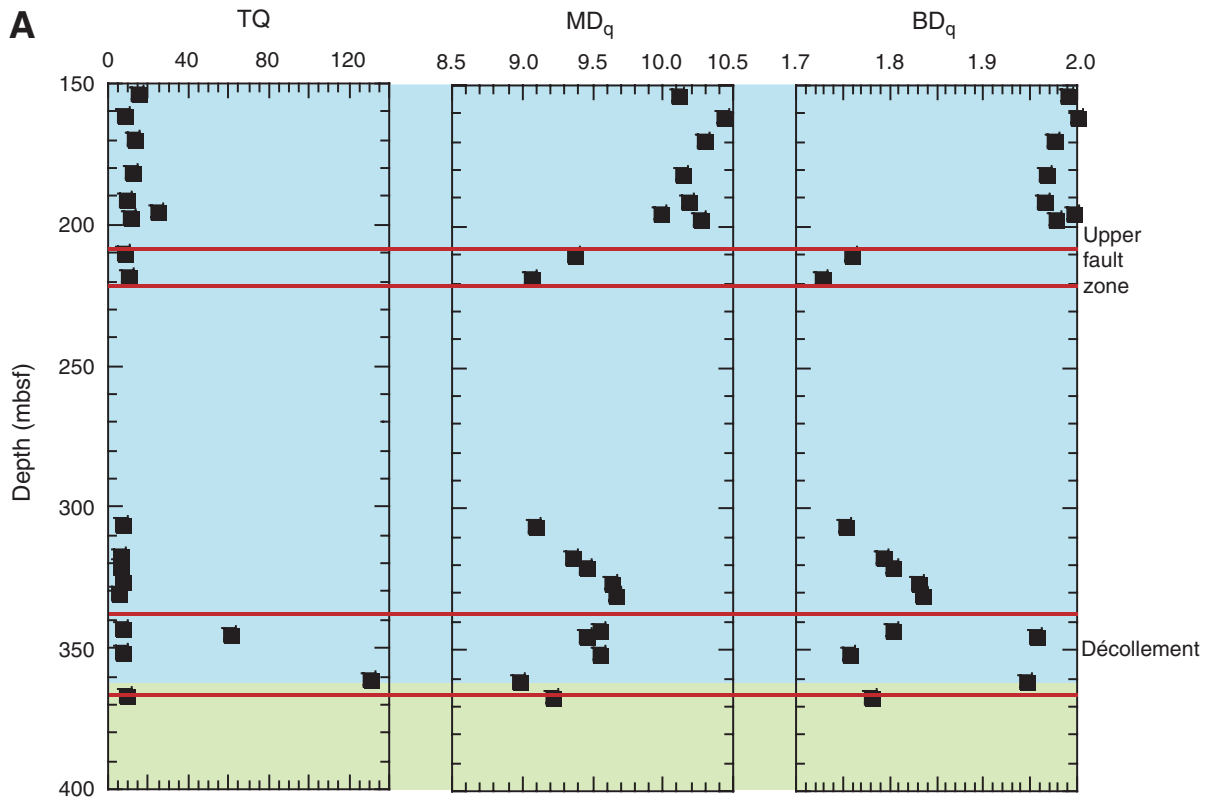
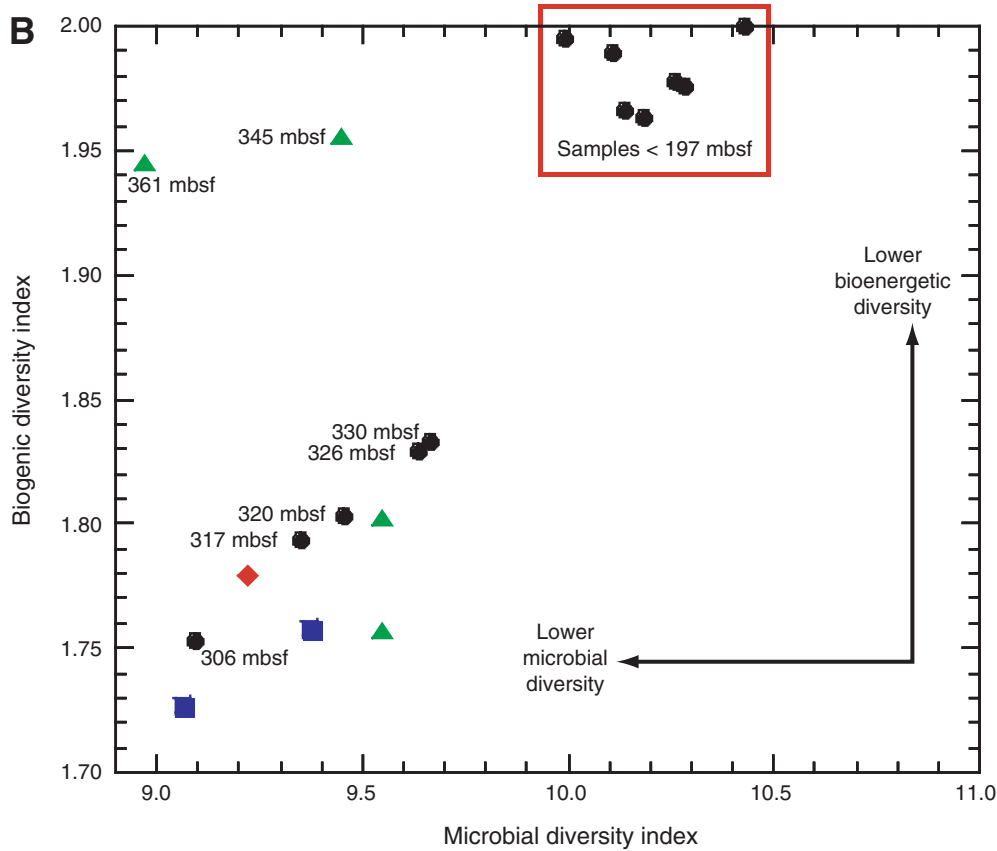


Figure F5 (continued). B.  $MD_q$ , plotted against bioenergetic divergence index for Site 1254 samples. Solid circles = samples not associated with fault structures at Site 1254. Approximate depths of samples are shown next to data points. Blue squares = two samples from within the heavily sheared zone in the upper prism, ~210–220 mbsf. Green triangles = four samples from within the décollement, ~338–364 mbsf. Red diamond = one sample from underthrust section.



**Table T1.** Biomarker data for sediment samples.

| Core, section,<br>interval (cm) | Depth<br>(mbsf) | DNA | M. gene<br>copy number<br>(cells/g solution)* | Measurement (pmol/g dry sediment) |      |       |       |       |       |      |      |       |      |      |      |         |      |       |
|---------------------------------|-----------------|-----|---|-----------------------------------|------|-------|-------|-------|-------|------|------|-------|------|------|------|---------|------|-------|
|                                 |                 |     |   | PLFA                              | UQ6  | UQ7   | UQ8   | UQ9   | UQ10  | MK4  | MK5  | MK6   | MK7  | MK8  | MK9  | Total Q | SSDL | UQ/MK |
| Incoming plate:                 |                 |     |   |                                   |      |       |       |       |       |      |      |       |      |      |      |         |      |       |
| 205-1253A-                      |                 |     |   |                                   |      |       |       |       |       |      |      |       |      |      |      |         |      |       |
| 1R-1, 13–29                     | 370.1           | –   | BDL   | BDL                               |      |       |       |       |       |      |      |       |      |      |      |         |      |       |
| 2R-2, 85–104                    | 377.9           | +   | BDL   | BDL                               | 0.29 | 0.3   | 0.33  | 0.38  | 0.36  | 0.21 | 0.22 | 0.24  | 0.17 | 0.15 | 0.14 | 2.77    | 0.14 | 1.47  |
| 3R-1, 7–23                      | 385.3           | +   | BDL   | BDL                               | 0.35 | 0.38  | 0.42  | 0.48  | 0.47  | 0.28 | 0.23 | 0.3   | 0.24 | 0.22 | 0.18 | 3.54    | 0.16 | 1.46  |
| 4R-3, 26–39                     | 398.2           | –   | BDL   | BDL                               | 0.35 | 0.38  | 0.36  | 0.44  | 0.43  | 0.2  | 0.2  | 0.25  | 0.2  | 0.18 | BDL  | 3.18    | 0.18 | 1.62  |
| 4R-3, 100–120                   | 398.9           | +   | BDL   | BDL                               |      |       |       |       |       |      |      |       |      |      |      |         |      |       |
| 5R-1, 0–1                       | 400.5           | –   | BDL   | BDL                               |      |       |       |       |       |      |      |       |      |      |      |         |      |       |
| 10R-2, 59–73                    | 431.3           | +   | BDL   | BDL                               | 0.18 | 0.2   | 0.19  | 0.22  | 0.24  | 0.14 | 0.13 | 0.14  | 0.1  | 0.1  | 0.09 | 1.72    | 0.1  | 1.47  |
| 11R-1, 81–96                    | 436.9           | +   | 931.3   | 13.37                             | 0.47 | 0.49  | 0.48  | 0.57  | 0.58  | 0.47 | 0.3  | 0.37  | 0.29 | 0.26 | BDL  | 4.5     | 0.24 | 1.35  |
| Forearc:                        |                 |     |   |                                   |      |       |       |       |       |      |      |       |      |      |      |         |      |       |
| 205-1254A-                      |                 |     |   |                                   |      |       |       |       |       |      |      |       |      |      |      |         |      |       |
| 1R-3, 47–52                     | 153.5           | +   | BDL   | 1.53                              | 0.6  | 0.79  | 1.41  | 1.71  | 1.73  | 1.8  | 0.69 | 3.28  | 1.28 | 0.98 | 0.32 | 14.57   | 0.09 | 0.75  |
| 2R-4, 120–125                   | 161.2           | +   | 1382.9  | BDL                               | 0.49 | 0.53  | 0.83  | 0.9   | 0.91  | 0.68 | 0.35 | 1.32  | 0.63 | 0.56 | 0.18 | 7.37    | 0.1  | 0.98  |
| 3R-3, 120–125                   | 169.3           | –   | BDL   | BDL                               | 0.7  | 0.58  | 1.03  | 1.28  | 1.35  | 1.52 | 0.84 | 2.8   | 1.19 | 1.03 | 0.32 | 12.66   | 0.09 | 0.64  |
| 4R-5, 90–95                     | 181.6           | –   | BDL   | BDL                               | 0.55 | 0.51  | 0.95  | 1.08  | 1.19  | 1.7  | 0.71 | 2.72  | 0.99 | 0.83 | 0.31 | 11.52   | 0.07 | 0.59  |
| 5R-5, 90–95                     | 190.8           | –   | BDL   | 0.45                              | 0.36 | 0.37  | 0.59  | 0.8   | 0.94  | 1.2  | 0.51 | 1.9   | 0.71 | 0.73 | 0.25 | 8.35    | 0.05 | 0.58  |
| 6R-1, 115–121                   | 195.3           | –   | BDL   | 0.66                              | 0.88 | 2.09  | 3.16  | 3.78  | 3.64  | 1.72 | 0.88 | 4.61  | 1.92 | 1.54 | 0.43 | 24.65   | 0.08 | 1.22  |
| 6R2, 166–171                    | 197.4           | +   | 230.3   | BDL                               | 0.49 | 0.53  | 0.86  | 1.22  | 1.18  | 1.39 | 0.74 | 2.31  | 0.97 | 0.9  | 0.26 | 10.85   | 0.08 | 0.65  |
| 7R-5, 74–79†                    | 209.9           | –   | BDL   | BDL                               | 0.39 | 0.24  | 0.26  | 0.26  | 0.21  | 1.85 | 0.74 | 1.95  | 0.97 | 0.64 | 0.33 | 7.86    | 0.06 | 0.21  |
| 8R-4, 45–50†                    | 218.1           | –   | BDL   | BDL                               | 0.49 | 0.29  | 0.3   | 0.31  | 0.22  | 3.06 | 1.14 | 2.35  | 1    | 0.6  | 0.5  | 10.25   | 0.07 | 0.19  |
| 9R-5, 40–45                     | 305.9           | –   | BDL   | BDL                               | 0.35 | 0.21  | 0.2   | 0.24  | 0.2   | 2.03 | 0.66 | 1.71  | 0.7  | 0.46 | 0.23 | 6.98    | 0.06 | 0.21  |
| 10R-6, 40–45                    | 317.1           | –   | BDL   | BDL                               | 0.3  | 0.19  | 0.19  | 0.2   | 0.18  | 1.57 | 0.54 | 1.17  | 0.5  | 0.39 | 0.17 | 5.41    | 0.06 | 0.24  |
| 11R-1, 117–123                  | 320.5           | –   | BDL   | BDL                               | 0.37 | 0.21  | 0.22  | 0.21  | 0.18  | 1.48 | 0.52 | 1.39  | 0.58 | 0.53 | 0.19 | 5.87    | 0.05 | 0.25  |
| 11R-5, 103–108                  | 326.1           | +   | 423.1   | 9.47                              | 0.38 | 0.23  | 0.25  | 0.26  | 0.32  | 1.62 | 0.61 | 1.44  | 0.68 | 0.55 | 0.2  | 6.53    | 0.06 | 0.28  |
| 12R-1, 141–148                  | 330.3           | +   | 432.1   | BDL                               | 0.28 | 0.18  | 0.17  | 0.2   | 0.18  | 1.18 | 0.46 | 0.89  | 0.48 | 0.35 | 0.14 | 4.52    | 0.06 | 0.29  |
| 13R-3, 145–150‡                 | 342.9           | –   | BDL   | BDL                               | 0.34 | 0.24  | 0.24  | 0.27  | 0.23  | 1.61 | 0.65 | 1.5   | 0.67 | 0.57 | 0.21 | 6.54    | 0.08 | 0.25  |
| 13R-5, 109–114‡                 | 345.1           | +   | BDL   | BDL                               | 2.15 | 7.37  | 12.15 | 8.3   | 9.37  | 1.35 | 1.02 | 10.3  | 3.81 | 3.79 | 1.16 | 60.78   | 0.1  | 1.84  |
| 14R-3, 40–45‡                   | 351.2           | –   | BDL   | BDL                               | 0.31 | 0.23  | 0.21  | 0.24  | 0.2   | 1.62 | 0.64 | 1.44  | 1    | 0.51 | 0.44 | 6.84    | 0.07 | 0.21  |
| 15R-3, 44–50‡                   | 361.1           | –   | BDL   | 1.62                              | 4.38 | 16.03 | 26.4  | 18.05 | 21.79 | 2.49 | 1.41 | 25.95 | 5.84 | 6.79 | 1.41 | 130.54  | 0.12 | 1.97  |
| 16R-3, 89–94                    | 366.6           | –   | BDL   | BDL                               | 0.46 | 0.28  | 0.27  | 0.31  | 0.25  | 2.6  | 0.8  | 1.8   | 0.75 | 0.65 | 0.26 | 8.43    | 0.08 | 0.23  |
| 205-1255A-                      |                 |     |   |                                   |      |       |       |       |       |      |      |       |      |      |      |         |      |       |
| 2R-2, 43–48                     | 134.4           | +   | BDL   | 4.14                              | 1.96 | 12.2  | 19.36 | 16.11 | 14.45 | 2.07 | 1.06 | 7.46  | 2.78 | 2.63 | 0.63 | 80.7    | 0.1  | 3.86  |
| 3R-2, 127–133                   | 145.2           | +   | BDL   | 14.89                             | 0.71 | 1.7   | 2.8   | 2.31  | 3.26  | 0.5  | 0.42 | 2.3   | 1.03 | 0.99 | 0.4  | 16.41   | 0.09 | 1.91  |
| 1255A-DF2R                      | –               | –   | BDL   | BDL                               | 0.73 | 0.83  | 0.79  | 0.96  | 0.93  | 0.74 | 0.73 | 0.56  | 0.53 | 0.42 | 0.37 | 7.58    | 0.37 | 1.26  |
| 1254A-DF1R                      | –               | –   | BDL   | BDL                               | 2.01 | 2.14  | 2.23  | 2.76  | 2.63  | 3.19 | 1.87 | 2.57  | 2.03 | 1.39 | 1.1  | 23.92   | 0.95 | 0.97  |
| 1254A-DF15R                     | –               | –   | BDL   | BDL                               | 1.43 | 1.48  | 1.42  | 1.73  | 1.68  | 1.83 | 1.01 | 1.4   | 1.01 | 0.78 | 0.69 | 14.46   | 0.69 | 1.15  |

Notes: DNA data are qualitative results from fluorescent screening. \* = methanogen-specific gene copy numbers/g solution (i.e., sediment extract), which is equivalent to cells/g solution. BDL = below detection limit. UQ = ubiquinones, MK = menaquinones, n = the number of isoprenyl units present in the side chain of the quinone core structure. Q = quinones. SSDL = sample-specific detection limit. UQ/MK = ratio of total UQ to total MK. Sample 205-1255A-2R-2, 43–48 cm, contains drilling slurry. † = sample from upper fault zone, ‡ = sample from décollement. Samples 1255A-DF2R, 1254A-DF1R, and 1254A-DF15R, so named for their relationship to drilling fluid (DF) and core of interest, are biomarker results obtained from lyophilizing ~50 mL of fluid collected on the catwalk as it ran from the retrieved core. This fluid is dominated by seawater.

**Table T2.** PLFA data for those samples that showed presence of at least one PLFA.

| Hole:                             | 205-1254A-     |                |                  |                   |                 | 205-1255A-     |                  | 205-1253A-      |
|-----------------------------------|----------------|----------------|------------------|-------------------|-----------------|----------------|------------------|-----------------|
|                                   | 1R-3,<br>47-52 | 5R-5,<br>90-95 | 6R-1,<br>115-121 | 11R-5,<br>103-108 | 15R-3,<br>44-50 | 2R-2,<br>43-48 | 3R-2,<br>127-133 | 11R-1,<br>81-96 |
| Core, section,<br>interval (cm):  |                |                |                  |                   |                 |                |                  |                 |
| Sample mass (g):                  | 10.8373        | 20.8329        | 12.9978          | 15.85             | 8.469           | 9.8255         | 11.1108          | 4.1932          |
| Dilution:                         | 25             | 25             | 25               | 25                | 25              | 25             | 25               | 25              |
| Total PFLA (pmol/g dry sediment): | 1.53           | 0.45           | 0.66             | 9.47              | 1.62            | 4.14           | 14.89            | 13.32           |
| PFLA component:                   |                |                |                  |                   |                 |                |                  |                 |
| 13:0 tridecanoic acid             | 0.00           | 0.00           | 0.00             | 3.20              | 0.00            | 0.00           | 0.00             | 0.00            |
| i14:0 iso-tetradecanoic acid      | 0.00           | 0.00           | 0.00             | 1.53              | 0.00            | 0.00           | 0.00             | 0.00            |
| 14:0 tetradecanoic acid           | 0.00           | 0.00           | 0.00             | 9.11              | 24.68           | 0.00           | 0.00             | 0.00            |
| i15:0 iso-pentadecanoic acid      | 0.00           | 0.00           | 0.00             | 4.31              | 0.00            | 0.00           | 0.00             | 0.00            |
| a15:0 antero-pentadecanoic acid   | 0.00           | 0.00           | 0.00             | 5.00              | 0.00            | 0.00           | 0.00             | 0.00            |
| 15:0 pentadecanoic acid           | 0.00           | 0.00           | 0.00             | 9.69              | 0.00            | 0.00           | 0.00             | 0.00            |
| i16:0 iso-hexadecanoic acid       | 0.00           | 0.00           | 0.00             | 3.95              | 0.00            | 0.00           | 0.00             | 0.00            |
| 16:0 hexadecanoic acid            | 50.86          | 8.18           | 0.00             | 35.40             | 51.13           | 68.33          | 78.20            | 86.03           |
| i17:0 iso-heptadecanoic acid      | 0.00           | 0.00           | 0.00             | 2.54              | 0.00            | 0.00           | 0.00             | 0.00            |
| 17:0 heptadecanoic acid           | 23.04          | 48.95          | 100.00           | 7.77              | 24.19           | 0.00           | 7.18             | 0.00            |
| 18:0 octadecanoic acid            | 26.10          | 42.87          | 0.00             | 13.70             | 0.00            | 31.67          | 14.62            | 13.97           |
| 20:0 dodecanoic acid              | 0.00           | 0.00           | 0.00             | 3.80              | 0.00            | 0.00           | 0.00             | 0.00            |

Notes: Sample 205-1255A-2R-2, 43-48 cm, contains drilling slurry. All other samples showed no detectable PLFAs.



**Table T3.** Quinone indexes for all sediment samples obtained during Leg 205.

| Core, section,<br>interval (cm) | Depth<br>(mbsf) | Total quinones<br>(pmol/g dry sediment) |       |       | MD <sub>q</sub> | BD <sub>q</sub> |
|---------------------------------|-----------------|---|-------|-------|-----------------|-----------------|
|                                 |                 | All                                     | UQ    | MK    |                 |                 |
| 205-1253A-                      |                 |   |       |       |                 |                 |
| 1R-1, 13–29                     | 370.13          |   |       |       |                 |                 |
| 2R-2, 85–104                    | 377.95          | 2.771                                   | 0.595 | 0.405 | 10.718          | 1.982           |
| 3R-1, 7–23                      | 385.27          | 3.540                                   | 0.593 | 0.407 | 10.733          | 1.983           |
| 4R-3, 26–39                     | 398.16          | 3.184                                   | 0.618 | 0.382 | 10.675          | 1.972           |
| 4R-3, 100–120                   | 398.9           |   |       |       |                 |                 |
| 5R-1, 0–1                       | 400.5           |   |       |       |                 |                 |
| 10R-2, 59–73                    | 431.31          | 1.716                                   | 0.595 | 0.405 | 10.731          | 1.982           |
| 11R-1, 81–96                    | 436.91          | 4.503                                   | 0.574 | 0.426 | 10.756          | 1.989           |
| 205-1254A-                      |                 |   |       |       |                 |                 |
| 1R-3, 47–52                     | 153.47          | 14.572                                  | 0.427 | 0.573 | 10.107          | 1.989           |
| 2R-4, 120–125                   | 161.2           | 7.37                                    | 0.496 | 0.504 | 10.429          | 2.000           |
| 3R-3, 120–125                   | 169.3           | 12.66                                   | 0.391 | 0.609 | 10.283          | 1.976           |
| 4R-5, 90–95                     | 181.56          | 11.517                                  | 0.371 | 0.629 | 10.138          | 1.966           |
| 5R-5, 90–95                     | 190.8           | 8.351                                   | 0.366 | 0.634 | 10.184          | 1.963           |
| 6R-1, 115–121                   | 195.25          | 24.654                                  | 0.55  | 0.450 | 9.989           | 1.995           |
| 6R-2, 166–171                   | 197.38          | 10.846                                  | 0.394 | 0.606 | 10.26           | 1.977           |
| 7R-5, 74–79                     | 209.95          | 7.859                                   | 0.174 | 0.826 | 9.372           | 1.758           |
| 8R-4, 45–50                     | 218.1           | 10.251                                  | 0.157 | 0.843 | 9.066           | 1.727           |
| 9R-5, 40–45                     | 305.9           | 6.979                                   | 0.171 | 0.829 | 9.092           | 1.753           |
| 10R-6, 40–45                    | 317.13          | 5.407                                   | 0.196 | 0.804 | 9.352           | 1.793           |
| 11R-1, 117–123                  | 320.47          | 5.873                                   | 0.202 | 0.798 | 9.456           | 1.803           |
| 11R-5, 103–108                  | 326.07          | 6.528                                   | 0.221 | 0.779 | 9.636           | 1.830           |
| 12R-1, 141–148                  | 330.31          | 4.523                                   | 0.224 | 0.776 | 9.666           | 1.833           |
| 13R-3, 145–150                  | 342.95          | 6.544                                   | 0.202 | 0.798 | 9.546           | 1.803           |
| 13R-5, 109–114                  | 345.09          | 60.783                                  | 0.647 | 0.353 | 9.451           | 1.956           |
| 14R-3, 40–45                    | 351.21          | 6.839                                   | 0.174 | 0.826 | 9.549           | 1.757           |
| 15R-3, 44–50                    | 361.09          | 130.543                                 | 0.664 | 0.336 | 8.971           | 1.945           |
| 16R-3, 89–94                    | 366.59          | 8.434                                   | 0.187 | 0.813 | 9.219           | 1.779           |
| 205-1255A-                      |                 |   |       |       |                 |                 |
| 2R-2, 43–48                     | 134.37          | 80.699                                  | 0.794 | 0.206 | 8.627           | 1.809           |
| 3R-2, 127–133                   | 145.17          | 16.412                                  | 0.656 | 0.344 | 9.757           | 1.950           |
| 1255A-DF2R                      |                 | 7.580                                   | 0.558 | 0.442 | 10.783          | 1.993           |
| 1254A-DF1R                      |                 | 23.919                                  | 0.492 | 0.508 | 10.792          | 2.000           |
| 1254-DF15R                      |                 | 14.461                                  | 0.535 | 0.465 | 10.764          | 1.997           |
| <i>Thermococcus zilligii</i>    |                 | 17.234                                  | 0.606 | 0.394 | 10.720          | 1.977           |
| <i>Paleococcus helgesonii</i>   |                 | 13.900                                  | 0.611 | 0.389 | 10.699          | 1.975           |
| Archaeal culture-AP             |                 | 33.105                                  | 0.629 | 0.371 | 10.639          | 1.966           |

Notes: Sample 205-1255A-2R-2, 43–48 cm, reflects drilling slurry contents. UQ = ubiquinones, MK = menaquinones. MD<sub>q</sub> = microbial divergence index, BD<sub>q</sub> = bioenergetic divergence index.

**Table T4.** Eigenvalues and eigenvectors associated with principal component analyses on correlations of quinones.

| Site:               | Sites 1253,<br>1254, and 1255 |       | Site 1254 |       |
|---------------------|-------------------------------|-------|-----------|-------|
|                     | PC1                           | PC2   | PC1       | PC2   |
| Eigenvalue:         | 9.31                          | 1.25  | 9.58      | 1.19  |
| Percent:            | 84.64                         | 11.38 | 87.07     | 10.79 |
| Cumulative percent: | 84.64                         | 96.02 | 87.07     | 97.86 |
| Eigenvectors:       |                               |       |           |       |
| UQ6                 | 0.32                          | -0.11 | 0.32      | -0.08 |
| UQ7                 | 0.32                          | -0.16 | 0.32      | -0.1  |
| UQ8                 | 0.32                          | -0.16 | 0.32      | -0.11 |
| UQ9                 | 0.31                          | -0.16 | 0.32      | -0.11 |
| UQ10                | 0.32                          | -0.17 | 0.32      | -0.11 |
| MK4                 | 0.15                          | 0.78  | 0.11      | 0.85  |
| MK5                 | 0.26                          | 0.52  | 0.27      | 0.46  |
| MK6                 | 0.32                          | -0.03 | 0.32      | -0.04 |
| MK7                 | 0.32                          | 0.02  | 0.32      | -0.06 |
| MK8                 | 0.32                          | -0.06 | 0.32      | -0.09 |
| MK9                 | 0.31                          | 0.03  | 0.31      | 0.02  |

Notes: Site 1253, 1254, and 1255 columns include combined data from all sediment samples at those sites; Site 1254 columns include data on sediment samples from that site only. PC1 = principal component 1, PC2 = principal component 2. UQ = ubiquinone, MK = menaquinone.